Inductance Gradient Variation With Time and Armature Sliding Along the Rails

Asghar Keshtkar, Shahab Mozaffari, and Ahmad Keshtkar

***Abstract*—The inductance gradient is one of the important parameters on the design and evaluation of railgun performance. The size, shape, and material of rails have effects on the inductance gradient. In 2-D analysis, the length of rails assumed to be infinite and then the effect of the armature ignored and a constant inductance gradient is obtained. In 3-D simulations, with assuming a fixed position for the armature (usually in the middle of rail), the inductance gradient can be determined. However, with the moving of the armature along rail length and the increasing of the current path, the applied force on the projectile will be different when it is constant and in the middle of the structure. Therefore, inductance gradient in the structure length will be changed. In this paper, with considering a railgun with copper rails with 1-m length, according to the input current and the resultant force of the aluminum armature in the rail length it was displaced in every step, the inductance gradient was determined. The results show that the amount of inductance gradient is not constant and will be increased with armature movement toward the muzzle.**

***Index Terms*—Inductance gradient, railgun, 3-D finite element method.**

I. Introduction

One electromagnetic launcher is a structure that with applying current to the rails, the armature between the two rails is accelerated and will be projected with a very high velocity. The inductance gradient of the railgun and the current density distribution in its structure is very important. The size, shape, and material of rails have effects on the inductance gradient. The amount of inductance gradient was obtained using 2-D analytical railgun models. [1].

Also, the effect of rail size (its cross section) on the current distribution and inductance gradient has been studied [2]. Furthermore, there is a report of inductance gradient calculation using 3-D simulations [3].

In 3-D simulations, with keeping constant the armature (usually in the middle of structure), they tried to calculate the applied force because of the current stimulation. Because of the movement of the armature along the rail length, the current path will be increased gradually. Therefore, the applied force to the armature in the beginning of movement will be different when the armature is in the middle of the structure or it is near the muzzle. Thus, inductance gradient is varying when the armature is moving from the breech to the muzzle, and when the armature is in the middle of structure.

Manuscript received January 13, 2010; revised April 11, 2010; accepted June 23, 2010. Date of publication August 23, 2010; date of current version January 7, 2011.

A. Keshtkar is with Imam Khomeini International University, Ghazvin 31546-15157, Iran (e-mail: akeshtkar@gmail.com).

S. Mozafari is with Computer and Electrical Engineering, University of Tabriz, Tabriz 51666-16471, Iran.

A. Keshtkar is with Medical Physics Department, Medical School, Tabriz University of Medical Sciences, Tabriz 51664, Iran.

Color versions of one or more of the figures in this paper are available online at http://ieeexplore.ieee.org.

Digital Object Identifier 10.1109/TPS.2010.2058131

A. Governing Equations

In the electromagnetic launcher function, there is an interference of several phenomena that are simultaneous and coupled with each other. The electromagnetic analysis of the railgun is complex, and its simulation needs more time. The differential equation for the potential of the magnetic vector $\vec{A}$ in the transient state is [4]

$$\nabla \times \left(\frac{1}{\mu}\nabla\times \vec{A}\right) + \sigma\frac{\partial \vec{A}}{\partial t} = \vec{J} \tag{1}$$

$$\nabla\times \vec{A} = \vec{B} \tag{2}$$

$\vec{B}$ is the magnetic flux density, μ is the permeability, σ is the electrical conductivity, and $\vec{J}$ is the applied current density. The interaction between the magnetic field density produced by the rail's current in the place of the armature and the passing current of the armature causes its acceleration in the rail length. This force is obtained from the Lorentz law

$$\vec{F} = \vec{J}\times \vec{B}\,. \tag{3}$$

By assuming that the applied force to the armature in the projectile axis is known, the inductance gradient of the structure is found from (4) as

$$L' = 2(F/I^2). \tag{4}$$

where F is the applied force to the armature in motion axis, and I is the input current.

B. Structure of the Railgun and Input Current

We choose the material of the rail to be copper, and the rail shape is a rectangular cube with a 0.5-cm width, 2-cm height, and 1-m length. The armature is a rectangular cube 1 cm wide, of the same height as the rail, and 8 mm long, and its material is aluminum. We model only a quarter of the structure because of the symmetry. Elements of the railgun structure are shown in Fig. 1.

In the electromagnetic projectiles, the stimulated current is very high, and this occurs usually with a capacitor discharging in two sides of the rail, and its shape will be the same as a

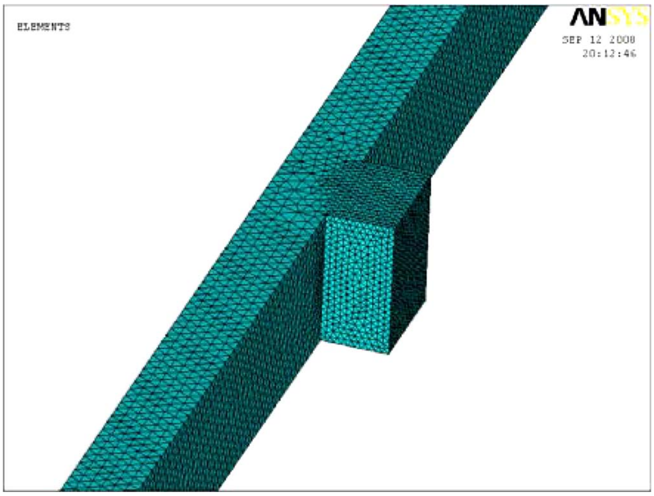

Fig. 1. Three-dimensional model of the rail and armature elements.

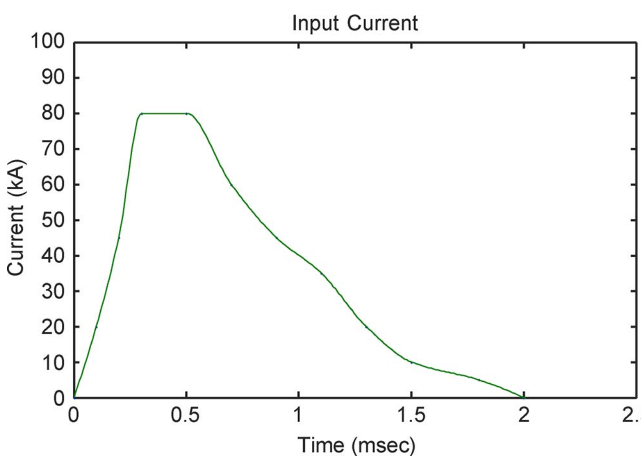

Fig. 2. Input current pulse.

pulse. Therefore, we consider a stimulated current using the simulation in Fig. 2. Whereas in 0.3 ms it reaches from 0 to 80 KA maximum, and it remains in the maximum amount about 0.2 ms, and then it reduces exponentially till $t = 2$ ms, then it approaches to zero.

II. Material Method and Simulation Results

A. Material Method

First of all, the armature is fixed 6 cm from the breech, and we assume that it is at rest to calculate the inductance gradient of the structure in the rail length. We divided the input current to a number of elements then by applying every part of input current, we calculate the applied force on the armature in the movement length. Thus, the inductance gradient can be obtained from (4). Therefore, by considering the applied force on the armature, the amount of its acceleration, velocity, and displacement is obtained. The armature is fixed in the new position for applying the other part of current stimulation. The flow chart of method is shown in Fig. 3. Thus, for applying every part of input current, we have to construct the structure and solve it again. We used the ANSYS software to solve its structure.

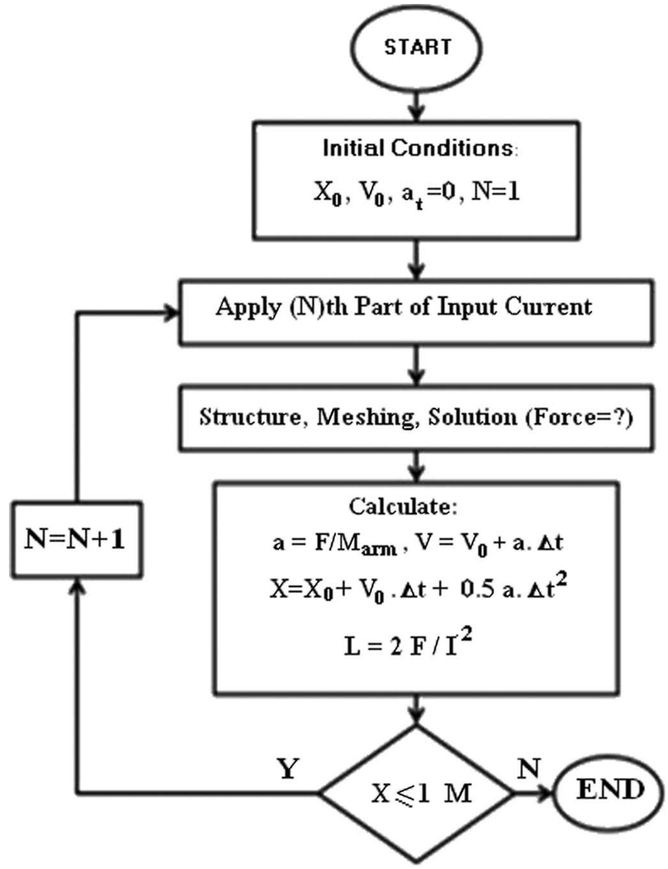

Fig. 3. Method flowchart.

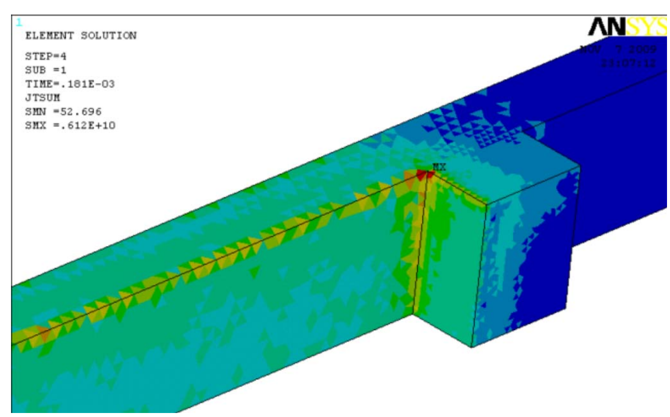

Fig. 4. Current density distribution of railgun at $t = 0.7$ ms.

B. Simulation Results

The current density distribution in the railgun when the input stimulation amplitude is 62 KA is shown in Fig. 4 (in the time of $t = 0.7$ ms). It is believed that the current density on the edge of the rail and the armature is concentrated. In the armature, the current density in the root area is very high, but the maximum current density is in the end edge of the rail connection.

The applied force on the railgun is in the x, y, and z-axes and is shown in Fig. 5. A force in the opposite of the rails is applied to the armature in the projectile axis (x-axis). In the y-axis so, the applied force on the rails can be pushed upwards or downwards. If the rail wide is not sufficient, it can cause its

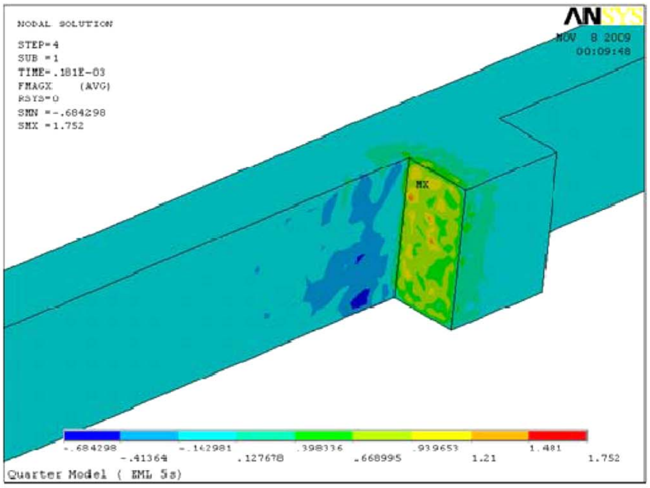

(a)

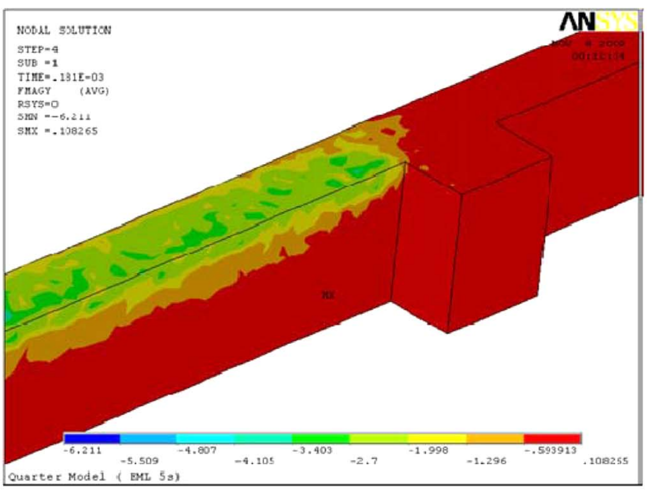

(b)

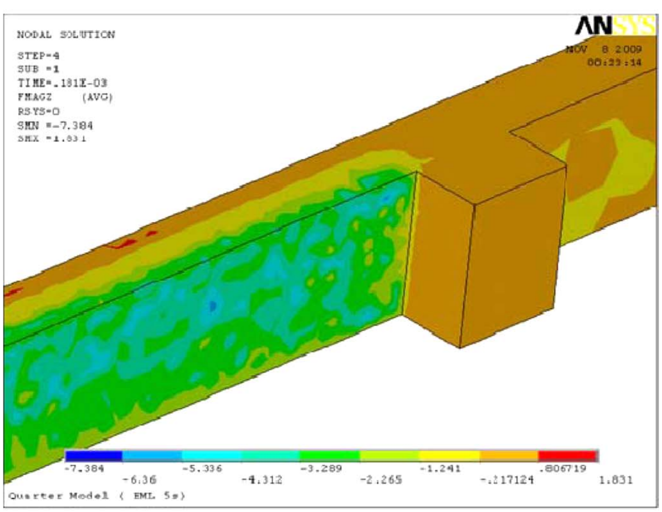

(c)

Fig. 5. Applied force on railgun at $t = 0.7$ ms (a) F_X. (b) F_Y. (c) F_Z.

deformation. The force applied to the rails in the z-axis so is expected to repel the rails from each other.

The applied force on the armature at $t = 0.7$ ms that is shown in Fig. 6 is demonstrated from the front and top views. The armature at the root region is under pressure and of course, the main part of the running force is in this region. In the rail

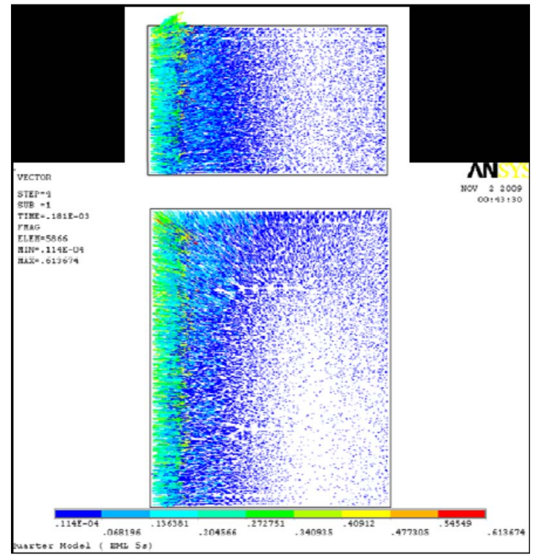

Fig. 6. Applied force on the armature at $t = 0.7$ ms. Down: front view. Up: top view.

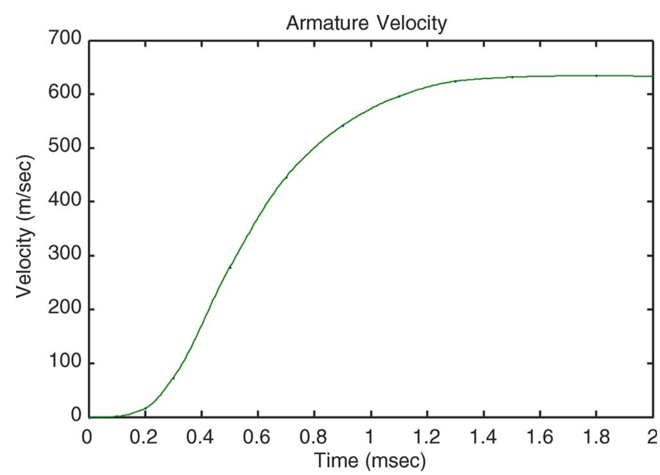

Fig. 7. Armature velocity.

contact border with the armature, it is seen that the armature is extended toward the rail.

The armature velocity current is shown in Fig 7.

The armature velocity near the muzzle is about 640 m/s. The inductance gradient variation in time and so in position of the armature is shown in Fig. 8 and 9. In Fig. 8, the inductance gradient is increased through time till $t = 1.5$ ms where it will be $L'_{\max} = 0.574$ μH. Then, the amount of the inductance gradient will be decreased. This can be because of edge effects. The amount of the inductance gradient in the beginning of movement is low. In Fig. 9, L' in the armature position is shown that at far points of edges, the variation of L' is light. In general, for far points of edges, it is shown that the inductance gradient at the rail axis is increased.

Since there was no published work using in these study sizes, we have simulated the structure in [3] to evaluate our results. In [3], Hsieh showed the effects of rail/armature geometry on the current distribution density and L'. Rails were made of copper and have a 2-cm height and 5-cm width. Also, the armature was made of aluminum with a 2-cm width, 2-cm height, and

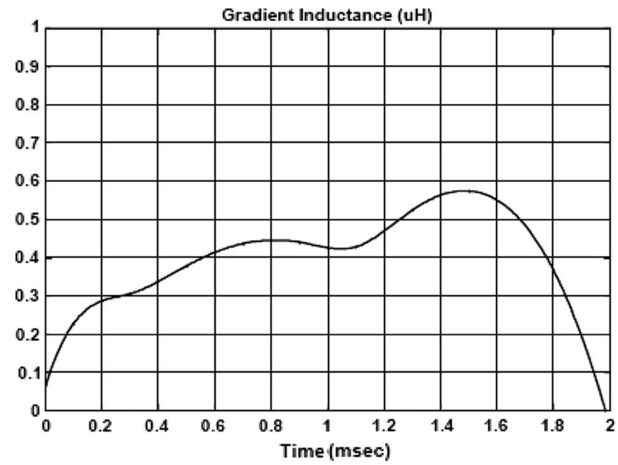

Fig. 8. Variation of inductance gradient in time.

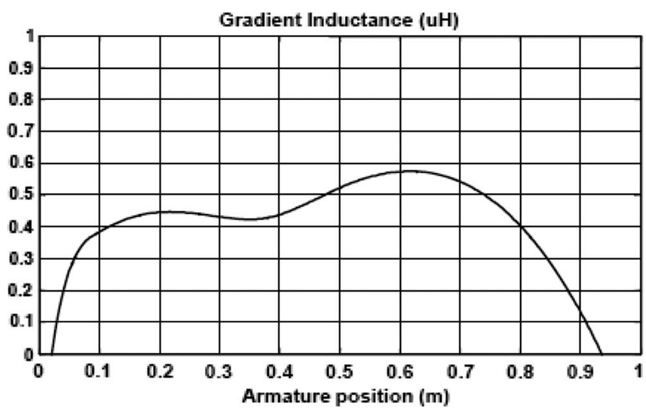

Fig. 9. Variation of inductance gradient during rail length.

1.8-cm length. To reduce the volume of calculation, only 1/4 of structure was simulated. The rail length was assumed to be 50 cm. By applying a current pulse with an amplitude of 50 KA, the force on the armature and the current distribution in the interface of the rail/armature calculated at $t = 10$ ms. Hsieh compared his work with the 2-D analytical model of Kerrisk, and because in this model he assumed that the current was without a high-frequency component, he selected the time $t = 10$ ms in the comparison of results. In Fig. 10(a), the current density distribution in the interface of the rail/armature is shown, and it demonstrated a good relation with the results of Hsieh in Fig. 10(b). The predicted amount of gradient inductance by the analytical method of Kerrisk is 0.529 μH. In the work done by Hsieh using the EMAP3D software, the gradient inductance is 0.525 μH. The results of the simulation using the ANSYS software show that the gradient inductance of 0.533 μH and the difference with Hsieh's and Kerrisk's results is less than 1%.

III. Conclusion

In the design and evaluation of the electromagnetic projectile function, considering a constant amount for the inductance gradient is not suitable because the amount of the inductance gradient of the rail is not constant. It increases with rail length and distance from the edges. The evaluation of the railgun when

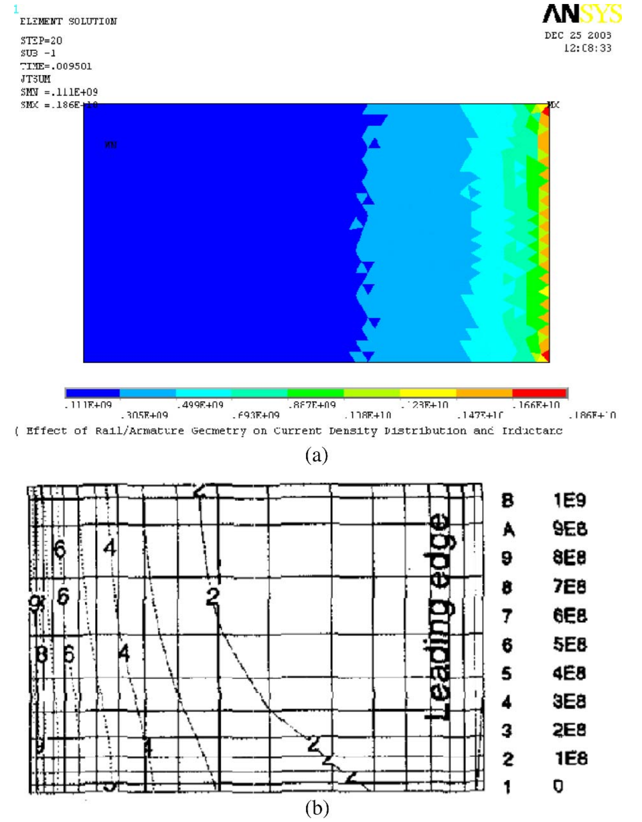

Fig. 10. Current distribution in the interface of the rail/armature (a) by Ansys and (b) by Hsieh [3].

the armature is displaced in the rail length makes possible the study of length variation effects of structure on the inductance gradient, the output velocity, and the current distribution. There are a few works that may be done in the future, such as considering the effect of narrowing the rail toward the muzzle and changing the rail conductivity on the projectile length path that can cause good effects on railgun function.

References

[1] F. Kerrisk, "Current Distribution and Inductance Calculation for Railgun Conductor," Los Alamos Nat. Lab., Los Alamos, NM, Rep. LA-9092-MS, Oct. 1980.
[2] A. Keshtkar, "Effect of rail dimension on current distribution and inductance gradient," *IEEE Trans. Magn.*, vol. 41, no. 1, pp. 383–386, Jan. 2005.
[3] B. K. Kim and K. T. Hsieh, "Effect of rail/armature geometry on current density distribution and inductance gradient," *IEEE Trans. Magn.*, vol. 35, no. 1, pp. 413–416, Jan. 1999.
[4] K. T. Hsieh, "A Lagrangian formulation for mechanically, thermally coupled electromagnetic diffusive processes with moving conductors," *IEEE Trans. Magn.*, vol. 31, no. 1, pp. 604–609, Jan. 1995.

Asghar Keshtkar was born in Ardabil, Iran, in 1962. He received the B.Sc. degree in electrical engineering from Tehran University, Tehran, Iran, in 1989, the M.Sc. degree in electrical engineering from the University of Khaje-Nasir, Tehran, in 1992, and the Ph.D. degree in electrical engineering from the Iran University of Science and Technology, Tehran, in 1999.

He is currently an Associate Professor with the Faculty of Engineering and Technology, Imam Khomeini International University, Ghazvin, Iran. His research interests include electromagnetic launcher, bioelectromagnetics, and antenna.

Shahab Mozaffari was born in Ravansar, Kermanshah, Iran, in 1985. He received the B.Sc. degree in electric and electrical engineering from Shahid Rajace Teacher Training University, Tehran, Iran, in 2006, and the M.Sc. degree in communication field and wave engineering from the University of Tabriz, Tabriz, Iran, in 2008.

He is currently with the Faculty of Electrical and Computer Engineering, University of Tabriz. His research interests include electromagnetic launcher, antenna, and neural networks.

Ahmad Keshtkar was born in Ardabil, Iran, in 1958. He received the B.Sc. degree in applied physics (solid state) from Shahid Beheshti University, Tehran, Iran, the M.Sc. degree in medical physics from Tarbiat-e-Modarres University, Tehran, and the Ph.D. degree in medical physics and engineering from the University of Sheffield, Sheffield, U.K., in 2004. His Ph.D. dessertation focused on the electrical impedance spectroscopy of the human urinary bladder to characterize this organ to find a minimally invasive technique for bladder cancer diagnosis.

He is currently an Associate Professor with the Medical Physics Department, Tabriz University of Medical Sciences, Tabriz, Iran. His major field of study is tissue characterization using electrical impedance spectroscopy.

Dr. Keshtkar is a member of the Iranian Association of Medical Physicists and a member of International Society For Electrical Bio-impedance (www.isebi.org).